Laser and Particle Beams

cambridge.org/lpb

Electron energy optimization by plasma density ramp in laser wakefield acceleration in bubble regime

M. Kaur and D. N. Gupta

Department of Physics and Astrophysics, University of Delhi, Delhi 110 007, India

Research Article

Cite this article: Kaur M, Gupta DN (2018). Electron energy optimization by plasma density ramp in laser wakefield acceleration in bubble regime. *Laser and Particle Beams* **36**, 195–202. https://doi.org/10.1017/S0263034618000162

Received: 14 November 2017
Revised: 14 May 2018
Accepted: 20 May 2018

Key words:
Bubble regime; dephasing length; laser wakefield acceleration

Author for correspondence:
D. N. Gupta, Department of Physics and Astrophysics, University of Delhi, Delhi 110 007, India.
E-mail: dngupta@physics.du.ac.in

Abstract

Energy gain of electron beams in bubble regime of the laser wakefield accelerator can be optimized by improving the acceleration length, radial accelerating and focusing force, number of monoenergetic electrons trapped inside the bubble, and increasing dephasing length. In order to enlarge the dephasing length, the phase velocity of the plasma wave can be increased by optimizing the plasma density profile. We report the estimation of dephasing length using plasma density distribution with the flat and linear-upward profile using two-dimensional particle-in-cell simulations. The size of wakefield bubble depends on the plasma density. With a positive plasma density gradient, the size of bubble decreases. The front and trail part of wake bubble will have different phase velocity in plasma density gradient region. After density transition in constant density region, the bubble elongates and the velocity of the back part of the bubble increases so that the accelerated electron phase synchronizes with the phase of the plasma wave. In a result, the electron acceleration length enhances to improve the beam quality.

Introduction

The state-of-the-art compact laser technologies have made laser wakefield acceleration (LWFA) scheme (Tajima and Dawson, 1979; Leemans *et al.*, 2006; Hafz *et al.*, 2008; Esarey *et al.*, 2009), an excellent and powerful tool for industrial, medical, and other applications. The interaction of short and intense laser pulse with plasma drives a plasma wave (Kaur and Gupta, 2016) that can trap and accelerate the electrons to relativistic energy over centimeter scales. The dynamics of accelerated electron bunch is determined by the properties of laser and plasma density. The high acceleration gradient, low-cost, and table-top size as compared with RF-based accelerators have enabled LWFA scheme, a promising technology for next-generation accelerators and compact radiation sources (Jaroszynski *et al.*, 2006; Nakajima, 2008; Albert *et al.*, 2014).

One of the most important issues in LWFA is the quality and stability of the electron beam. The energy gain, emittance, and spread of accelerated electron bunch are regulated by the longitudinal and transverse injection mechanism of electrons (Dawson, 1959; Faure *et al.*, 2004; Geddes *et al.*, 2004; Mangles *et al.*, 2004; Tsung *et al.*, 2004). Various methods have been proposed for injecting electrons into the wakefield including density transition (Schimd *et al.*, 2010) or density downramp injection (Hansson *et al.*, 2015), ionization-induced injection (Yu *et al.*, 2014), colliding optical injection (Davoine *et al.*, 2009). But the self-injection scheme is preferred more in designing the accelerators as there is no need for external injector. The self-injection mechanism in bubble regime of LWFA offers a possibility in generating high-energy electron beam and has been investigated theoretically (Kostyukov *et al.*, 2009; Benedetti *et al.*, 2013; Lee *et al.*, 2015) and experimentally (Hafz *et al.*, 2011; Banerjee *et al.*, 2013) in recent years.

Pukhov and Meyer-ter Vehn (2002) presented the self-injection of electrons in the bubble regime of laser wakefield using particle-in-cell (PIC) simulations. The bubble regime of laser wakefield accelerator is characterized by an ultrashort laser pulse with $a_0 \geq 4$ and pulse length shorter than the plasma wavelength ($c\tau_0 \leq r_0 \approx 2\sqrt{a_0}c/\omega_p$), where τ_0, r_0, and a_0 are laser pulse duration, spot size, and normalized vector potential, respectively, and ω_p and c are plasma frequency and speed of light, respectively. Using three-dimensional (3D)-PIC simulations, Lu *et al.* (2007) have shown that the LWFA in bubble regime can be operated even if $2 \leq a_0 \leq 4$, where the bubble radius (R) matches with the spot size of the laser pulse such that $k_pR \approx k_pr_0 = 2\sqrt{a_0}$ (where k_p is the plasma wave number). The ponderomotive force of ultrashort laser pulse expels the plasma electrons, leaving ions behind and forming a cavity devoid of electrons called "bubble". This bubble is demonstrated as 3D plasma wave trailing behind the laser pulse that moves at relativistic speeds. The electric field due to charge separation will trap the electrons at the back of the bubble and accelerate them to higher energy. These

© Cambridge University Press 2018

CAMBRIDGE UNIVERSITY PRESS

electrons can outrun the plasma wave and move into a decelerating region to lose energy. Theoretically, it has been observed that the evolution of bubble structure determines the quality of the accelerated electron bunch (Kalmykov *et al.*, 2011; Li *et al.*, 2015; Toosi *et al.*, 2016).

To improve the electron bunch quality, it is important to control the laser as well as the plasma parameters, improve the diagnostic techniques, and improve the total acceleration distance, which is limited by diffraction, depletion, and dephasing length. Extension of laser–plasma interaction length has been achieved through the combination of performed plasma channel guiding, relativistic self-focusing, and ponderomotive self-channeling to mitigate the problem of diffraction (Sprangle *et al.*, 1996; Kaur *et al.*, 2017). Self-guiding provides stability to the bubble evolution, and hence controls the self-injection enabling the production of extremely high-quality electron bunch (Kalmykov *et al.*, 2010). One of the major limitations in achieving monoenergetic electron beam in LWFA is dephasing between plasma wave and electron beam due to the difference between the velocity of accelerated electrons and the phase velocity of the wakefield. The length over which the electron travels before it gets decelerated is called the dephasing length. The dephasing length limitation can be mitigated by lowering the plasma density, but sufficient plasma density is required for self-injection to occur.

The profile of plasma density is very important in LWFA experiments and it should be considered in a way to synchronize for the accelerated electron corresponding to the phase velocity of the bubble. The dephasing length in bubble regime (L_d) is calculated from the phase velocity of the plasma wave (υ_φ) and the bubble radius (R) as $L_d = R/(1 - \upsilon_\varphi/c)$. Katsouleas (1986) was the first to propose a way to overcome the dephasing limitation by tailoring the plasma density, commonly referred as plasma tapering. The tapering mechanism to phase lock a relativistic particle by the accelerating (longitudinal field) and focusing (transverse field) forces have been studied theoretically by Rittershofer *et al.* (2010). Bulanov *et al.* (1998) performed 1D-PIC simulations of a laser pulse with propagating in a downward plasma density ramp and found that the plasma wave breaks on the ramp and injects a significant number of electrons. Albeit, the electrons are accelerated to high energy, but the energy spread of the electron bunch is very large. Kim *et al.* (2011) simulated the effect of upward plasma density ramp on energy gain of electrons through a 2D-PIC code for a 20 TW laser and observed that, in case of upward plasma density ramp, the acceleration region moves faster as compared with the downward ramp and uniform plasma density. The plasma wave generates a higher accelerating gradient to generate an energetic electron bunch. Yu *et al.* (2015) has theoretically analyzed the phase velocity of wakefield and estimated the threshold required to achieve the self-injection by introducing linear up-ramp plasma density gradient and verified it using PIC simulations. However, the scaling laws for the plasma density ramp still need to be investigated to optimize the bubble parameters to estimate the electron energy gain.

The strong ponderomotive force of a high-intensity laser pulse ($a_0 \geq 4$) interacting with an underdense plasma ($\omega_p^2 << \omega^2$) expels all the electrons, creating an ion cavity called the bubble, with electrons acting as sheath boundary. The plasma electrons at the rear of the bubble get self-injected and accelerated due to the corresponding longitudinal electric field of the bubble. These electrons gain energy while propagating with the velocity close to the speed of light. For highly non-linear regime, the phase velocity of a plasma wave is calculated from the laser pulse front velocity considering the laser pulse depletion effect. In case of uniform plasma, the bubble velocity at the front and rear remains same throughout, which is equal to the phase velocity of the plasma wave, i.e. $\upsilon_\varphi \approx \upsilon_g - \upsilon_{etch} \approx c(1 - 3n_e/2\gamma n_c)$, where $\upsilon_g = c(1 - n_e/2\gamma n_c)$ is the group velocity of laser pulse, and $\upsilon_{etch} \approx n_e/\gamma n_c$ is the etching velocity due to laser pulse depletion. n_e and n_c are the plasma density and the critical density, respectively, and $\gamma = \sqrt{1 + a_0^2/2}$. The accelerated electron will get out of the phase after traveling a certain distance called dephasing length. The difference in the velocities of plasma wave and accelerated electron accounts for dephasing. In order to suppress dephasing, a positive linear-upward density profile is introduced in this proposal such that the bubble shrinks leading to difference in the front and back velocities of the bubble.

In this paper, we examined the improvement in dephasing length and energy gain of the accelerated electrons by introducing a linear-upward density ramp structure in bubble regime of LWFA by performing 2D-PIC simulations using VORPAL code (Nieter and Cary, 2004). We have considered upward plasma density ramp with different ramp lengths followed by a uniform density region and measured the effect of density ramp length on the phase velocity of bubble wake leading to an increase in dephasing length and energy gain of the accelerated electrons. We have elucidated the physics of dephasing length in bubble regime to study its dependence on the linear-upward plasma density distribution. The 2D-PIC simulations have been proposed to investigate the effect of linear-upward density profile on dephasing length and energy gain followed by the conclusion.

Two-dimensional PIC simulations

We have performed 2D-PIC simulations using VORPAL simulation code to optimize the dephasing length and the electron energy gain by considering linear-upward plasma density profile. A linearly polarized laser pulse propagates along x-direction with a transverse electric field of $\mathbf{E} = \hat{z}E_0 \exp(-x^2/L_{rms}^2) \exp(-r^2/r_0^2) \cos(\omega t - kx)$ in a plasma of length of 1500 μm. The full width at half maximum (FWHM) laser pulse τ_0 is related as $L_{rms} = c\tau_0/\sqrt{8 \ln 2}$. The laser pulse strength is $a_0 = 5$ with the wavelength of $\lambda = 0.8$ μm, the spot size of $r_0 = 9$ μm, and the pulse duration of $\tau_0 = 30$ fs (FWHM). The focus of laser pulse is fixed in the middle of the density ramp. The plasma density profile is defined over a distance with different upward density ramp length ranging from 0 to 700 μm over which the density is increased from 0 to $n_e = 4 \times 10^{25}$ m^{-3} followed by a flat density plateau such that the total plasma length is the sum of the ramp and flat length. A moving window is used for simulation with window size resolved in x- and y-directions with grid size $\lambda/30$ and $\lambda/4$, respectively. The number of particles per cell used for simulations is four. The laser and plasma parameters are not exactly matched to the resonant condition of bubble regime in our simulations, but these are optimized for sufficient self-injection of the particles at the rear of the bubble to accelerate to higher energies. The evolution of laser pulse and coupling between the interacting waves has been neglected in this study. This may be justified by the fact of highly non-linear system ($a_0 > 4$) and, of course, the exact physics would also be really difficult to explore in that scenario. We have also performed simulations for a uniform plasma density case (i.e. no plasma density ramp). The results of this case have been compared with the case of plasma density ramp.

The schematic diagram of plasma density profile is shown in Figure 1 for four different cases by considering the flat density

https://doi.org/10.1017/S0263034618000162 Published online by Cambridge University Press

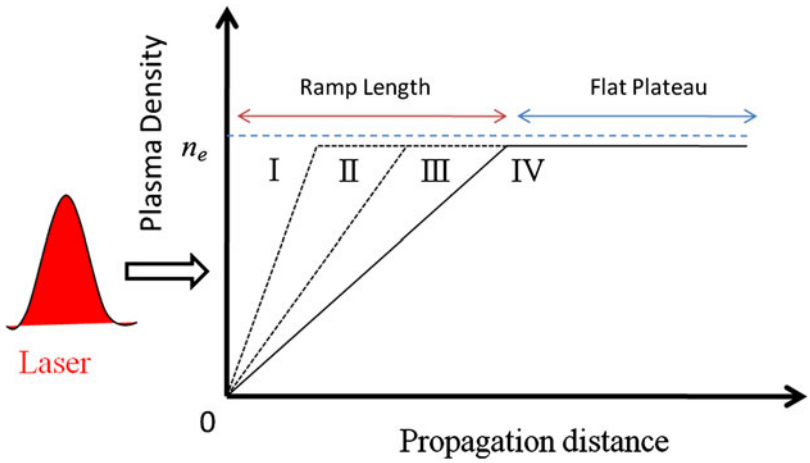


Fig. 1. Schematic representation of linear-upward plasma density distribution used in PIC simulation with ramp length (d_r) varied for four different cases: without ramp $d_r = 0$ (case I), and with ramp $d_r = 300$ μm (case II), $d_r = 500$ μm (case III), and $d_r = 700$ μm (case IV). The plasma density ramp is followed by the flat density plateau with a total plasma length of 1500 μm.

with no ramp, i.e. $d_r = 0$ (case I), upward ramp length of $d_r =$ 300 μm (case II), $d_r = 500$ μm (case III), and $d_r = 700$ μm (case IV). In all these cases, the density increases linearly from 0 to n_e for $0 \le x \le d_r$ and then remains constant at $n_e = 4 \times 10^{25}$ m^{-3} for $d_r \le x \le 1500$ μm. This kind of plasma density profile can be generated experimentally using a capillary gas cell and controlled by sending the gas with varying pressures at two inlets (Kim *et al.*, 2016). The gas density is increased from the capillary entrance by changing the pressure of the first inlet such that the density gradient is created along the capillary axis from the entrance to intersection of the capillary and second inlet, keeping a constant pressure.

An ion cavity (or bubble) is created due to the ponderomotive force of the laser pulse that expels all the electrons. The field generated in the bubble exerts the force on some of the unshielded electrons for self-injection to occur. These self-trapped electrons will undergo the process of acceleration to increase their energy. We have compared the contour plot of charge density distribution showing the formation of bubble and the self-injection of particles in Figure 2a–2d at same time $t = 1.8$ ps for all four cases. We have chosen the observation point at $t = 1.8$ ps to compare the evolution of bubble in all cases. The corresponding maximum energy gain of the accelerated electrons is shown in Figure 2e–2h. In case I (Fig. 2a), a stable bubble is formed after laser has propagated a distance of about 230 μm and the electrons are self-injected in the bubble. These self-injected electrons are accelerated continuously to a maximum energy of 0.16 GeV before these electrons outrun the plasma wave (Fig. 2e). The bubble structure elongated during the acceleration of self-injected electrons. A stable bubble is formed after density transition in case II. The acceleration of self-injected electrons after the formation of bubble and the corresponding energy gain of continuous accelerated electron beam are shown in Figure 2b and 2e, respectively. During the density transition, the plasma wavelength increases. When the laser pulse interacts with inhomogeneous plasma, the group velocity of the laser pulse is modified due to its dependence on the plasma wavelength. Consequently, the corresponding phase velocity of the wakefield and the radius of the bubble structure are also modified. The electrons accumulated at the back of the bubble are self-injected and accelerated to higher energies after attaining a certain threshold (Yu *et al.*, 2015). In case III (Fig. 2c), the bubble starts evolving at the end of ramp at 500 μm, where the electrons self-inject at the back of the bubble. These self-injected electrons are accelerated continuously to achieve maximum energy gain before they get decelerated. At time $t = 1.8$ ps, the bubble is fully evolved in cases I, II, and III. However, the same is not observed for case IV (Fig. 2d), where the ramp length is much larger (700 μm). During the density transition along the ramp length, the size of the bubble structure decreases and the self-injection does not occur. The density gradient should be sharp enough in order to modify the phase velocity of the bubble for self-injection to occur.

The energy gain of the accelerated electrons is sensitive to the length of plasma density ramp. A stable bubble is formed after the laser has traversed a distance equal to the density ramp length. Beyond this length, the bubble elongates in the longitudinal direction and the phase velocity of the back part of the bubble increases. The self-injected electrons are continuously accelerated as the phase velocity of the bubble synchronizes with the accelerated electron velocities. Consequently, the electrons gain higher energy during this process. The energy of electrons is enhanced with the dephasing length over which the electrons are accelerated.

For many applications, it is desirable to generate monoenergetic high-quality accelerated electron beam from the accelerators. Therefore, it is important to study the energy spectra of self-injected accelerated electrons. The energy spectrum of the accelerated electrons for all cases shown in Figure 3 is not monoenergetic due to the continuous injection of electrons. It has been previously studied that the self-focusing of the laser pulse results in the elongation of the bubble and improved self-injection of the electrons (Kim *et al.*, 2003). The evolution of bubble structure can be controlled by employing a density gradient in such a way that results in limiting the number and energy spread of the injected electrons. It can be predicted from the results that the peak energy gained by the number of particles is higher in case of plasma density ramp profile as compared with the case of flat density profile.

The energy spectra of the electrons having peak energy of 0.12 GeV, when a flat density distribution is considered, is not enviable for many applications. It is shown that the energy spread is reduced by employing an upward plasma density gradient in a plasma. This may be because the number of self-injected electrons increases due to enhanced self-focusing of laser pulse when a positive density gradient is considered over an upward ramp with a typical scale length of $3R_{d0}$ (Rayleigh length) (Gupta *et al.*, 2007). In our results, the electron beam is better collimated with a peak energy of 0.2 GeV (almost double) if a density ramp length of 700 μm is introduced. This is because of the reason that the ratio of longitudinal to transverse velocity of electrons is higher in this case. The accelerated electrons have both longitudinal and transverse velocities. The electrons, thus, are

https://doi.org/10.1017/S0263034618000162 Published online by Cambridge University Press

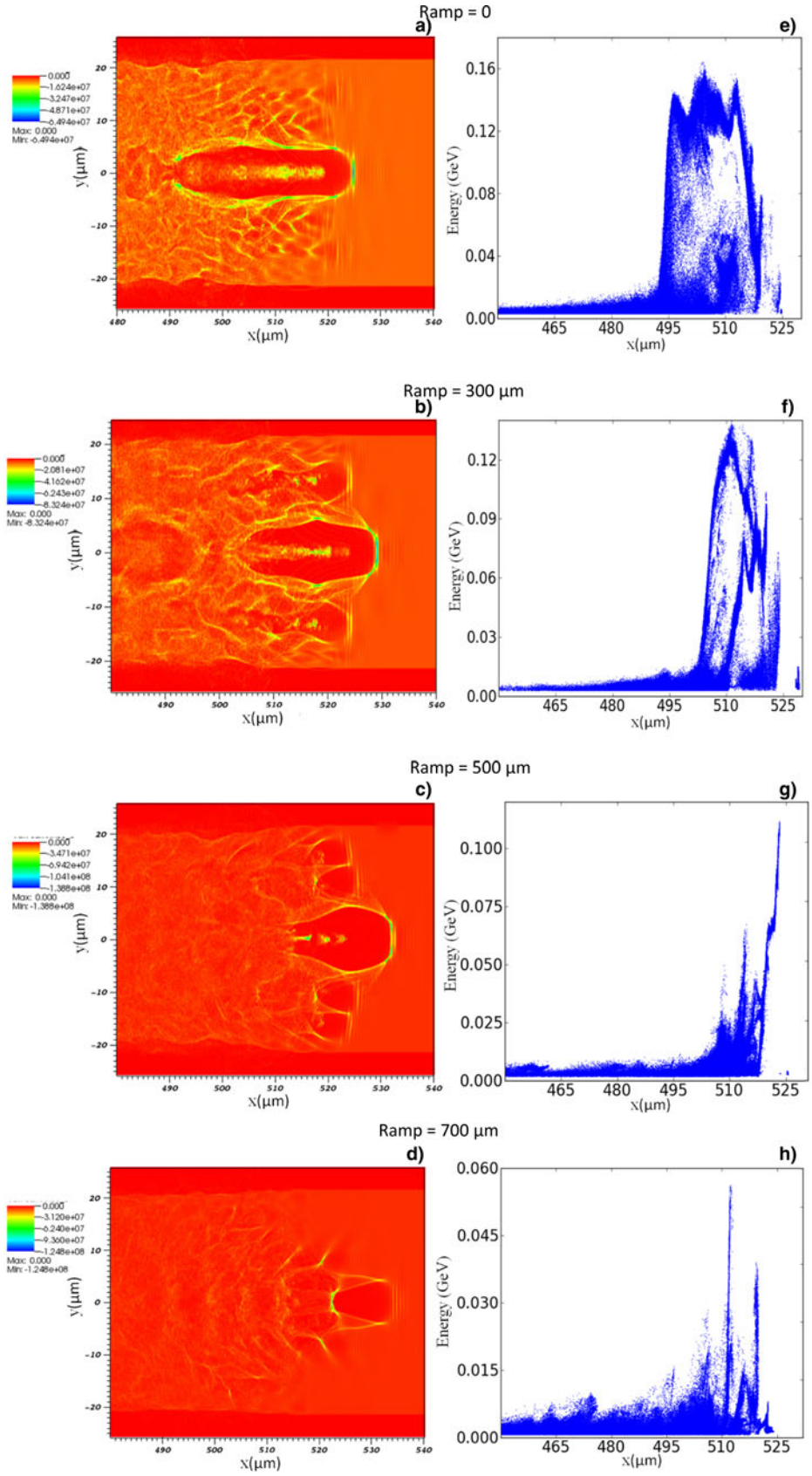


Fig. 2. Contour plot of charge density distribution (a–d) and maximum energy gain of accelerated electrons (e–h) in the case of linear-upward density profile with no ramp, and ramp length 300 μm, 500 μm, and 700 μm for $a_0 = 5$ at time $t = 1.8$ ps.

synchronized with the plasma wave resulting in a highly collimated electron beam. It has been observed in a number of simulations that if the ramp length (d_r) is larger than 500 μm, the electrons are self-injected before it reaches the maximum plasma density. This can be attributed to the fact that the threshold to achieve self-injection in non-linear regime varies for different

https://doi.org/10.1017/S0263034618000162 Published online by Cambridge University Press

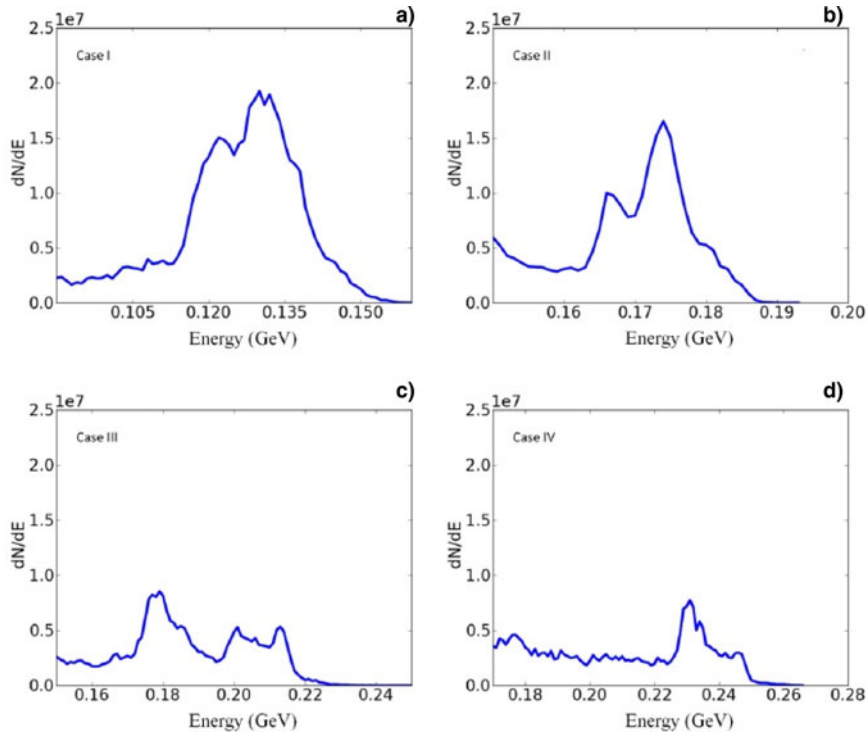


Fig. 3. Electron energy spectrum with different plasma density distribution for (a) flat density profile, (b) the plasma density ramp length of 300 μm, (c) the plasma density ramp length of 500 μm, and (d) the plasma density ramp length of 700 μm.

plasma density distribution as the phase velocity of the bubble modifies with the plasma density profile. So, it is important to choose the upward plasma density gradient appropriately for self-injection of electrons in LWFA.

The size of the bubble is a function of laser pulse intensity and plasma density. When an upward density ramp is introduced, the bubble shrinks with velocity $\upsilon_{sh} = -\lambda\,(d\sqrt{\gamma n_c/n_e}/dx)\upsilon_b$, where x and υ_b are the position and back velocity of the bubble and λ is the laser pulse wavelength (Decker and Mori, 1994; Wen *et al.*, 2010). The front velocity is same as the laser pulse group velocity. So, the bubble back velocity in terms of plasma density gradient can be expressed as $\upsilon_b = \upsilon_{sh} + \upsilon_\varphi \approx c(1 - 3n_e/2\gamma n_c)/(1 + \lambda\left(\sqrt{\gamma n_c}/n_e^{3/2}\right)dn_e/dx)$. This equation implies that the bubble back velocity increases with the plasma density to synchronize with electron velocity. Reversely, the front velocity of the bubble decreases due to pulse depletion.

In Figure 4, the charge density distribution showing the evolution of bubble structure and the corresponding energy gain of the accelerated electrons are observed at three different times $t =$ 1.7 ps, 2.3 ps, and 2.7 ps, where a plasma density gradient with a ramp length of 500 μm has been used. Initially, when a stable bubble is formed at the end of ramp length, the self-injected electrons get accelerated to only a few MeV (Fig. 4a and 4d). The bubble structure shrinks during the density transition region. When the laser has surpassed the ramp length and comes in the flat density region, the bubble excited by laser pulse elongates along the longitudinal direction as shown in Figure 4c. The change in the size of the bubble increases the back phase velocity while front velocity of bubble remains same. This assists more number of electrons to attain the self-injection threshold and thus a continuous acceleration may be reasonable to higher energies of the electrons. The maximum electron energy achieved in this case is about 0.24 GeV (Fig. 4f). The electrons get out of phase after traveling an acceleration distance equal to the dephasing length and lose energy as they enter the decelerating region.

In Table 1, using 2D-PIC simulations, we have tabulated the values of maximum dephasing length and the corresponding electron energy gain achieved in bubble regime of LWFA by employing different plasma density gradients with varying ramp lengths.

Enhancement in dephasing length and maximum energy achieved by the accelerated electrons with the ramp length of linear-upward density profile has been presented in Figure 5. When the flat density distribution of the plasma is considered, the dephasing length is about 290 μm, which is in close agreement with the calculated theoretical value for these laser and plasma parameters (Nakajima *et al.*, 2015). When a linear-upward density profile is introduced at the beginning of plasma such that the density increases from 0 to $n_e = 4 \times 10^{25}$ m^{-3} over a distance equal to the ramp length (d_r), the dephasing length is extended over larger distances. For highly non-linear regime ($a_0 = 5$), the length over which electrons get accelerated to higher energy is also extended due to an increase in dephasing length. The energy gain of the accelerated electrons is scaled with dephasing length. Hence, the energy gain is also enhanced by employing a linear up-ramp plasma density profile. For a plasma density profile with a ramp length of 900 μm, the dephasing length is extended to 430 μm and the corresponding maximum energy gain of the accelerated electrons is about 0.32 GeV.

Conclusion

In order to study the effects of plasma density distribution on dephasing length and accelerated electrons energy gain in bubble regime of laser wakefield accelerators, 2D-PIC simulations have been performed. We have optimized the laser and plasma parameters for sufficient self-injection of electrons in LWFA. The dephasing length limits the energy gain of accelerated electrons by reducing the acceleration length. The self-injected electrons get trapped and are accelerated to higher energies over a distance equal to the dephasing length until the electrons remain in phase

https://doi.org/10.1017/S0263034618000162 Published online by Cambridge University Press

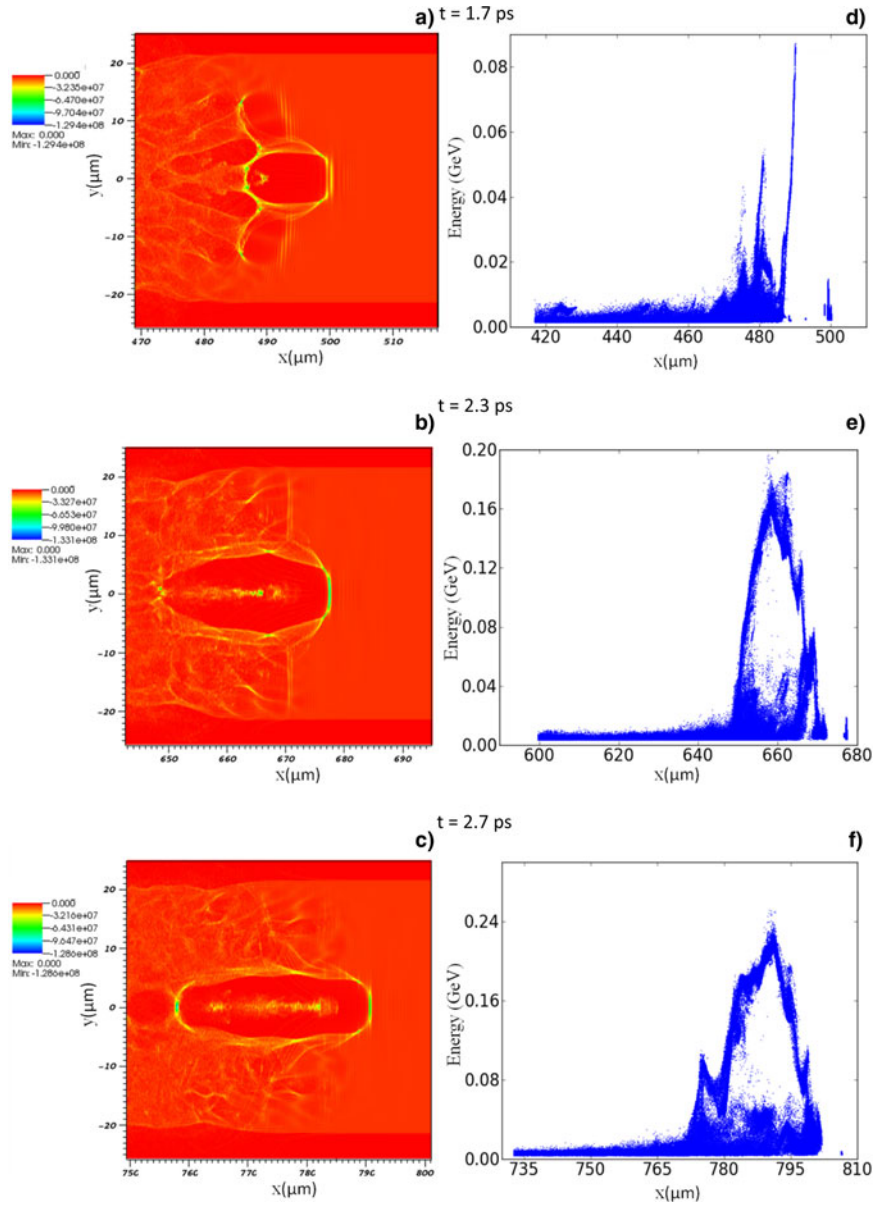


Fig. 4. Contour plot of charge density distribution (a–c) and corresponding energy gain of accelerated electrons (d–f) for upward density gradient plasma with ramp length of 500 μm at three different time steps $t = 1.7$ ps, 2.3 ps, and 2.7 ps.

Table 1. Dephasing length and electron energy gain optimization using PIC simulations

Density ramp length (μm)	Dephasing length (μm)	Electron energy gain (GeV)
0	290	0.16
300	300	0.18
500	320	0.24
700	400	0.26
900	430	0.32

with the plasma wave. After that distance, the electrons enter into the decelerating region and lose energy. In case of flat plasma density distribution, the maximum electron energy gain is about 0.16 GeV. In order to extend the dephasing length over longer distances, we have introduced a linear-upward density profile with different ramp length (d_r), over which the electron density starts from zero and attains a maximum value $n_e = 4 \times 10^{25}$ m^{-3} and then remains constant for the rest of the plasma region. It was observed that the dephasing length is extended over larger distances by considering the linear-upward density profile. The dephasing is generated because of the difference in the accelerated electron velocity and the phase velocity of the bubble. The front velocity of bubble matches with the laser pulse front velocity, while the back velocity of the bubble is increased during the density transition due to its dependence on plasma density gradient such that it synchronizes with the electrons moving with relativistic velocities. After the density gradient region, the bubble structure elongates in the longitudinal direction and an electron beam with enhanced energy gain due to extended dephasing length was observed. The energy gain of accelerated electrons is about 0.26 GeV in case of linear-upward plasma density profile of a ramp length of 700 μm. The energy spread of the accelerated electrons is also reduced by increasing the ramp length, since the number of self-injected electrons attaining threshold increases with larger

https://doi.org/10.1017/S0263034618000162 Published online by Cambridge University Press

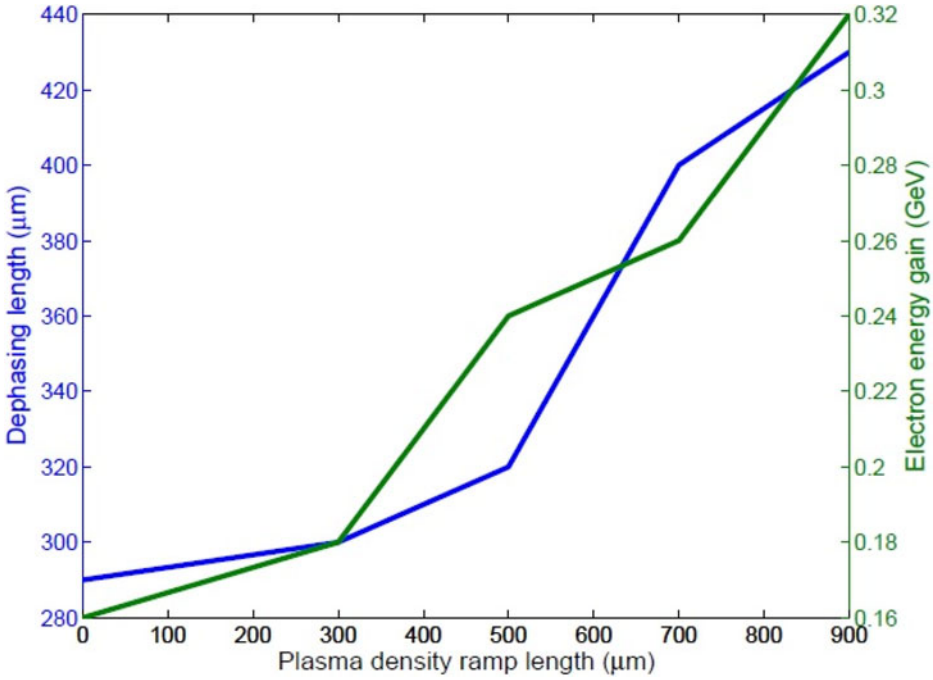


Fig. 5. Dephasing length (blue) and electron energy gain (green) with the ramp length (μm) for $a_0 = 5$, $r_0 = 9$ μm, and $\tau_0 = 30$ fs.

longitudinal velocities. The energetic electron beam is more collimated in the case of linear-upward density profile. This study may be crucial in understanding the role of plasma density profile to enhance the accelerated electron energy and controlling the electron beam collimation in bubble regime of LWFA.

Acknowledgement. This work was supported by the Department of Science and Technology, Govt. of India under DST-RFBR joint research proposal (Grant No. INT/RUS/RFBR/P-186).

References

Albert F, Thomas AGR, Mangles SPD, Banerjee S, Corde S, Flacco A, Litos M, Neely D, Vieiria J, Najmudin Z, Bingham R, Joshi C and Katsouleas T (2014) Laser wakefield accelerator based light sources: potential applications and requirements. *Plasma Physics and Controlled Fusion* **56**, 084015.

Banerjee S, Kalmykov SY, Powers ND, Golovin G, Ramanathan V, Cunningham NJ, Brown KJ, Chen S, Ghebregziabher I, Shadwick BA, Umstadter DP, Cowan BM, Bruhwiler DL, Beck A and Lefebvre E (2013) Stable, tunable, quasi-monoenergetic electron beams produced in a laser wakefield near the threshold for self-injection. *Physical Review ST Accelerators And Beams* **16**, 031302.

Benedetti C, Schroeder CB, Esarey E, Rossi F and Leemans WP (2013) Numerical investigation of electron self-injection in the nonlinear bubble regime. *Physics of Plasmas* **20**, 103108.

Bulanov S, Naumova N, Pegoraro F and Sakai J (1998) Particle injection into the wave acceleration phase due to nonlinear wake wave breaking. *Physical Review E* **58**, R5257–R5260.

Davoine X, Lefebvre E, Rechatin C, Faure J and Malka V (2009) Cold optical injection producing monoenergetic, multi-GeV electron bunches. *Physical Review Letters* **102**, 065001.

Dawson JM (1959) Nonlinear electron oscillations in a cold plasma. *The Physical Review* **113**, 383–387.

Decker CD and Mori WB (1994) Group velocity of large amplitude electromagnetic waves in a plasma. *Physical Review Letters* **72**, 490–493.

Esarey E, Schroeder CB and Leemans WP (2009) Physics of laser-driven plasma-based electron accelerator. *Reviews of Modern Physics* **81**, 1229–1285.

Faure J, Glinec Y, Pukhov A, Kiselev S, Gordienko S, Lefebvre E, Rousseau JP and Malka V (2004) A laser-plasma accelerator producing monoenergetic electron beams. *Nature* **431**, 541–544.

Geddes CGR, Toth Cs, van Tilborg J, Esarey E, Schroeder CB, Bruhwiler D, Nieter C, Cary J and Leemans WP (2004) High-quality electron beams from a laser wakefield accelerator using plasma-channel guiding. *Nature* **431**, 538–541.

Gupta DN, Hur MS, Hwang I, Suk H and Sharma A (2007) Plasma density ramp for relativistic self-focusing of an intense laser. *Journal of the Optical Society of America B: Optical Physics* **24**, 1155–1159.

Hafz NAM, Jeong TM, Choi IW, Lee SK, Pae KH, Kulagin VV, Jung JH, Yu TJ, Hong KH, Hosokai T, Cary JR, Ko DK and Lee J (2008) Stable generation of GeV-class electron beams from self-guided laser-plasma channels. *Nature Photonics* **2**, 571–577.

Hafz NAM, Lee SK, Jeong TM and Lee J (2011) Evolution of self-injected quasi-monoenergetic electron beams in a plasma bubble. *Nuclear Instruments & Methods in Physics Research. Section A, Accelerators, Spectrometers, Detectors and Associated Equipment* **637**, S51–S53.

Hansson M, Aurand B, Davoine X, Ekerfelt H, Svensson K, Persson A, Wahlstrom CG and Lundh O (2015) Down-ramp injection and independently controlled acceleration of electrons in a tailored laser wakefield accelerator. *Physical Review ST Accelerators and Beams* **18**, 071303.

Jaroszynski DA, Bingham R, Brunetti E, Ersfield B, Gallacher J, Van Der Geer B, Isaac R, Jamison SP, Jones D, De Loos M, Lyachev A, Pavlov V, Reitsma A, Saveliev Y, Vieux G and Wiggins SM (2006) Radiation sources based on laser-plasma interactions. *Philosophical Transactions of the Royal Society A* **364**, 689–710.

Kalmykov SY, Beck A, Yi SA, Khudik VN, Downer MC, Lefebvre E, Shadwick BA and Umstadter DP (2011) Electron self-injection into an evolving plasma bubble: quasi-monoenergetic laser-plasma acceleration in the blowout regime. *Physics of Plasmas* **18**, 056704.

Kalmykov SY, Beck A, Yi SA, Khudik V, Shadwick BA, Lefebvre E and Downer MC (2010) Electron self-injection into an evolving plasma bubble: the way to a dark current free GeV-scale laser accelerator. *AIP Conference Proceedings* **1299**, 174–179.

Katsouleas T (1986) Physical mechanisms in the plasma wake-field accelerator. *Physical Review A* **33**, 2056–2064.

Kaur M and Gupta DN (2016) Simulation of laser-driven plasma beat-wave propagation in collisional weakly relativistic plasmas. *Europhysics Letters* **116**, 35001.

https://doi.org/10.1017/S0263034618000162 Published online by Cambridge University Press

Kaur M, Gupta DN and Suk H (2017) Evolution of Laser pulse shape in a parabolic plasma channel. *Laser Physics* **27**, 015401.

Kim C, Kim GH, Kim JU, Ko IS, Lee HJ and Suk H (2003) Self-injection of electrons in evolution of wake wave. *Conference Proceedings of the PAC* **3**, 1852–1854.

Kim J, Kim GJ and Yoo SH (2011) Energy enhancement using an upward density ramp in laser wakefield acceleration. *Journal of the Korean Physical Society* **59**, 3166–3170.

Kim M, Lee S, Kim J, Nam I and Suk H (2016) Feasibility study of a laser-driven high energy electron acceleration in a long up-ramp density. *Conference Proceedings of the IPAC* **3**, 2576–2578.

Kostyukov I, Nerush E, Pukhov A and Seredov DV (2009) Electron self-injection in multidimensional relativistic-plasma wake fields. *Physical Review Letters* **103**, 175003.

Lee S, Lee TH, Gupta DN, Uhm HS and Suk H (2015) Enhanced betatron oscillations in laser wakefield acceleration by off-axis laser alignment to a capillary plasma waveguide. *Plasma Physics and Controlled Fusion* **57**, 075002.

Leemans WP, Nagler B, Gonsalves AJ, Toth C, Nakamura K, Geddes CGR, Esarey E, Schroeder CB and Hooker SM (2006) GeV electron beams from a centimeter-scale accelerator. *Nature Physics* **2**, 696–699.

Li XF, Yu Q, Gu YJ, Huang S, Kong Q and Kawata S (2015) Bubble shape and electromagnetic field in the nonlinear regime for laser wakefield acceleration. *Physics of Plasmas* **22**, 083112.

Lu W, Tzoufras M, Joshi C, Tsung FS, Mori WB, Vieiria J, Fonseca RA and Silva LO (2007) Generating multi-GeV electron bunches using single stage laser wakefield acceleration in a 3D nonlinear regime. *Physical Review ST Accelerators and Beams* **10**, 061301.

Mangles SPD, Murphy CD, Najmudin Z, Thomas AGR, Collier JL, Dangor AE, Divall EJ, Foster PS, Gallacher JG, Hooker CJ, Jaroszynski JA, Langley AJ, Mori WB, Norreys PA, Tsung FS, Viskup R, Walton BR and Krushelnick K (2004) Monoenergtic beams of relativistic electrons from intense laser-plasma interactions. *Nature* **431**, 535–538.

Nakajima K (2008) Compact X-ray sources: towards a table-top free-electron laser. *Nature Physics* **4**, 92–93.

Nakajima K, Kim H, Jeong T and Nam C (2015) Scaling and design of high-energy laser plasma electron acceleration. *High Power Laser Science* **3**, 1–11.

Nieter C and Cary JR (2004) VORPAL: a versatile plasma simulation code. *Journal of Computational Physics* **196**, 448–473.

Pukhov A and Meyer-Ter Vehn J (2002) Laser wake field acceleration: the highly non-linear broken-wave regime. *Applied Physics B: Lasers and Optics* **74**, 355–361.

Rittershofer W, Schroeder CB, Esarey E, Gruner FJ and Leemans WP (2010) Tapered plasma channels to phase-lock accelerating and focusing forces in laser-plasma accelerator. *Physics of Plasmas* **17**, 063104.

Schimd K, Buck A, Sears CMS, Mikhailova JM, Tautz R, Herrmann D, Geissler M, Krausz F and Veisz L (2010) Density-transition based electron injector for laser driven wakefield accelerators. *Physical Review ST Accelerators and Beams* **13**, 091301.

Sprangle P, Esarey E and Krall J (1996) Self-guiding and stability of intense optical beams in gases undergoing ionization. *Physical Review E* **54**, 4211.

Tajima T and Dawson JM (1979) Laser electron accelerator. *Physical Review Letters* **43**, 267–270.

Toosi ES, Mirzanejhad S and Dorronian D (2016) Bubble structure in laser wake-field acceleration. *Laser and Particle Beams* **34**, 193–201.

Tsung FS, Narang R, Mori WB, Joshi C, Fonseca RA and Silva LO (2004) Near-GeV-energy laser-wakefield acceleration of self-injected electrons in a centimeter-scale plasma channel. *Physical Review Letters* **93**, 185002.

Wen M, Shen B, Zhang X, Wang F, Jin Z, Ji L, Wang W, Xu J and Nakajima K (2010) Controlled electron acceleration in the bubble regime by optimizing plasma density. *New Journal of Physics* **12**, 045010.

Yu LL, Esarey E, Schroeder CB, Vay JL, Benedetti C, Geddes CGR, Chen M and Leemans WP (2014) Two-color laser-ionization injection. *Physical Review Letters* **112**, 125001.

Yu Q, Gu YJ, Li XF, Huang S, Kong Q and Kawata S (2015) Electron self-injection into the phase of a wake excited by a driver laser in a nonuniform density target. *Physics of Plasmas* **22**, 073107.

https://doi.org/10.1017/S0263034618000162 Published online by Cambridge University Press